JOURNAL OF MATERIALS SCIENCE **36** (2001) 3409–3414

Lateral stress measurements in a shock loaded alumina: Shear strength and delayed failure

J. C. F. MILLETT, N. K. BOURNE
Royal Military College of Science, Cranfield University, Shrivenham, Swindon, SN6 8LA, UK
E-mail: j.millett@rmcs.cranfield.ac.uk

Manganin gauges have been embedded in AD975 alumina in such orientation that renders them sensitive to the lateral component of stress during shock loading. A secondary increase in lateral stress, which indicates a decrease in overall shear strength has been observed. It has generally been assumed that such features are damage fronts. Gauges placed at increasing distances from the impact face show that the damage front penetrates less than 5 mm. It is believed that interactions with grain boundaries impede the fronts progress. With increasing impact stress, results show that the velocity of the damage front increases until failure occurs in the main shock itself. Such behaviour has been observed in other brittle materials such as silicon carbide and glasses.

1. Introduction

The properties of ceramics under one-dimensional shock-loading have been of interest for many years, either as light weight amour materials or as components for jet turbines. For example, materials such as boron carbide [1], silicon carbide [2] and titanium diboride [3] have all attracted attention. In this test geometry, a flat flyer plate of a known material is impacted upon a target that is carefully aligned to the flyer, such that the planarity of impact is to within 5 optical fringes (25 μm over 50 mm). At high impact velocities (>100 m s^{-1}), the impact launches a planar shock front into the target, behind which, conditions of one-dimensional-strain occur. In this situation (assuming of course that the material is isotropic), the strain (ε) is accommodated down the impact axis, whilst the strains perpendicular to it are zero, due to inertial confinement. In contrast, there must be a confining stress (σ_y) perpendicular to the impact axis, thus,

$$\varepsilon_x \neq 0 \neq \varepsilon_y = \varepsilon_z = 0 \text{ and } \sigma_x \neq \sigma_y = \sigma_z \neq 0. \quad (1)$$

The subscript x refers to the impact axis, whilst subscripts y and z are orientated orthoganly to x. For a more detailed discussion of the shock behaviour of materials, the reader is directed to the review article of Davison and Graham [4].

More specifically, the behaviour of alumina based ceramics under shock loading conditions has been the subject of investigation for the past three decades. Early work by Gust and Royce [1] showed that the Hugoniot Elastic Limit (HEL)—which can be related to the yield strength (Y) under conditions of one-dimensional stress through the Poisson's ratio, ν,

$$Y = \frac{1-2\nu}{1-\nu}\text{HEL}, \quad (2)$$

- varied from 6.1 to 13.4 GPa, depending upon precise composition. Their results showed that strength increased with increasing purity levels, presumably corresponding to the reduction of intergranular glassy phases.

A number of workers have addressed the phenomenon of elastic precursor decay, that is the apparent decrease in the HEL with specimen thickness until a steady value is reached. Gust and Royce [1] demonstrated this feature in both boron carbide and a hot pressed alumina. Murray *et al*. [5] have shown that precursor decay occurs over an alumina purity range, from 88% to 99.9%, although it was observed that it was a more dominant feature in the lower purity materials. Staehler *et al*. [6] also observed precursor decay in a high purity (99.9%) alumina. In contrast, Cagnoux and Longy [7] report no such decay in their material. The results of Grady [8] also suggest that precursor decay is not present in polycrystalline ceramics, although it should be pointed out that he takes his HEL at a different point in the loading histories (midway between the end of the elastic rise and the start of the plastic part of the shock front) than other workers [5, 6], simply at the break in slope. In general, it would seem that there is a difference in opinion about the existence of precursor decay in aluminas. On the one hand, those using manganin stress gauges supported on the back of the target with polymethylmethacrylate (PMMA) [5, 6, 9] show evidence that precursor decay is present, whilst those using VISAR (*v*elocity *i*nterferometer *s*ystem for *a*ny *r*eflector) [7, 8] suggest otherwise. Thus it would appear that some disagreement exists over the presence of precursor decay in aluminas. As the manganin stress gauges are backed with PMMA, it could be argued that they are susceptible to reverberations at the alumina/PMMA interface, whilst VISAR measurements, taken from the free surface are not. Currently, this is an

active area of research at this laboratory, with preliminary results indicating that gauges do indeed give an accurate measurement of the materials behaviour. Another factor that needs consideration is the microstructure. At a microscopic level, polycrystalline aluminas consist of differently orientated grains, and as such differing yield strengths that are dependent on orientation. However, the grain size of polycrystalline aluminas tends to be of the order of a few microns, whilst a typical manganin stress gauge has an area 4×4 mm^2. Thus it can be seen that the relatively large gauge size (compared to the grain size) will average out any individual responses from the grains and thus should give an average stress measurement that is representative of the bulk material behaviour. In contrast, the probe size of the VISAR is smaller, of the order of 1 mm^2, hence it could be argued that it is VISAR, not gauges that could be more vulnerable to variations in microstructure. In practice, the probe size is still much greater than the grain size and so microstructural effects are likely to be minimal. However, we do note with interest that the work of Gust and Royce [1], using high-speed-photograph measurements to monitor the free surface velocity did detect precursor decay in both boron carbide and some grades of alumina, although it should be pointed out that these results were published nearly thirty years ago.

Over that past decade, one of the more important features of the shock loading of brittle materials is the failure wave. This was first detected in K19 (similar to soda-lime) glass by Razorenov *et al*. [10]. In examining rear surface velocity traces (VISAR) in this material, they noticed the presence of small reloading signals superimposed upon the main velocity trace. They suggested that this was the result of the release from the rear of the target interacting with a slower moving front behind the main shock, but ahead of the release wave from the rear of the flyer plate. As this interaction was recorded as a reload signal, they deduced that the material behind this slow-moving front had undergone a reduction in shock impedance. If true, one possible mechanism could be a fracture process. This they dubbed the *failure wave*. Some time previously, Nikolaevskii [11] had proposed just such a mechanism to explain the behaviour of brittle materials during shock loading. However, as these reload signals tended to be difficult to detect, Kanel *et al*. [12] suggested that they might be detected by more direct means such as spall strength or lateral stress measurements. If the failure wave did represent a front behind which the material was damaged, then it might be expected that the spall (tensile) strength caused by the interaction of release waves from the rear of the target and flyer plate should reduce to zero. In addition, lateral stresses (σ_y) should show an increase, since the shear strength (τ) of any material under one-dimensional shock-loading is defined by the well known relation,

$$2\tau = \sigma_x - \sigma_y. \tag{3}$$

Brar and his colleagues [13–15] demonstrated that such behaviour did indeed occur, providing further conformation that the above hypothesis was correct. Bourne *et al*. [16] also provided evidence for failure waves via high-speed-photography, showing them as a front behind which both soda-lime and borosilicate glasses lost their opacity. In a recent series of papers, we have also shown that failure waves are also present in shock-loaded polycrystalline ceramics including silicon carbide [17], alumina [18] and titanium diboride [19]. Unlike glasses, where failure wave velocity was shown to be constant as it moved through the target [16], in ceramics [18] the velocity was shown to decrease as it progressed into the target, and in fact did not penetrate further than 5 mm. Here we suggested that grain boundaries may have impeded the progress of the failure wave. Bourne *et al*. [20] also made the observation that the distance over which the failure wave penetrates in a 97.5% alumina corresponded with the decay distance of the elastic precursor. They suggested that decay distance may infact refer to the stress at which the failed zone is formed, as measured by observations of the shear strength. Staehler *et al*. [6] observed that the elastic precursor in a 99.9% pure material reached a stable value only after 9 mm, more than the 5 mm quoted for the 97.5% alumina material. Presumably this would be due to differences in microstructure and composition. Failure waves have also been observed in other materials such as glass-ceramics [21], where their presence was detected by superimposed reload signals, in a manner similar to Razorenov *et al*. [10] Rosenberg and Yesherun [22] also detected reload signals in the manganin stress gauge traces from AD-85, an 85% purity commercial alumina. However, they did not interpret this as due to a failure wave, but rather the result of a fast compressional wave originating from flyer plate/specimen interface. Given the current state of knowledge, it would seem more likely that this recompression was indeed the result of a failure wave. Furnish and Chhabildas [23] also investigated the possibility of strength degradation in shocked alumina, by shock-reshock experiments such that the second shock was just above the materials HEL. Their results suggested that there was indeed some reduction (or relaxation in shear strength) due to the passage of the first shock wave. Brar [24] has reviewed the work on brittle materials from a number of laboratories, including glasses and polycrystalline ceramics where failure waves (delayed failure) has been deduced via a range of techniques. Grady [25] has also discussed the possibility of failure waves in ceramics, suggesting that an alternative pressure volume curve is initiated due to dilatancy caused by shear failure. Therefore it would seem that there is considerable evidence for failure waves in polycrystalline ceramics.

Finally, in a recent paper [26], we have demonstrated that the shear strength behind the failure wave has a direct bearing on a materials ballistic performance. In that paper, we showed that the ratio of the depth on penetration (DoP) in full ballistic impact experiments between alumina and titanium diboride were almost identical to the ratio of the shear strengths behind the failure wave in the same materials.

In this paper, we further investigate the shear strength of a 97.5% pure alumina, both at constant stress as a

function of distance from the impact surface, and at constant distance from the impact face as a function of impact stress.

2. Experimental

Plate impact experiments were carried out on a 50 mm bore, 5 m long, single stage gas gun [27]. Target plates of 97.5% alumina, dimensions 22 mm thick by 50 mm × 50 mm were sectioned in half, and manganin stress gauges (MicroMeasurements type J2M-SS-580SF-025) were introduced at various distances from the impact face. Targets were reassembled using a low viscosity epoxy adhesive with a curing time of ∼12 hours. The impact faces were lapped to a flatness of 5 optical fringes over 50 mm. Specimen configurations and gauge locations are shown in Fig. 1.

Voltage—time data from the gauges was reduced to lateral stress using the methods of Rosenberg and Partom [28], with a modified analysis that does not require knowledge of the longitudinal (impact) stress [29]. In doing so, we have followed the assumptions of Rosenberg and Partom [28] in that the lateral stress recorded by the gauge is the same as that experienced by the sample, and that there is no slippage between the gauge, the insulation around the gauge and the sample itself. We feel justified in doing so since in an earlier paper, Rosenberg *et al*. [30] in using strain gauges in shock loaded specimens, which are mounted in the same manner as the lateral stress gauges, measured the same strains as those calculated through the known shock relations. 10 mm copper flyer plates were impacted onto the targets in the velocity range 324 to 647 m s^{-1}, so as to induce impact stresses in the range 6.3 to 12.5 GPa.

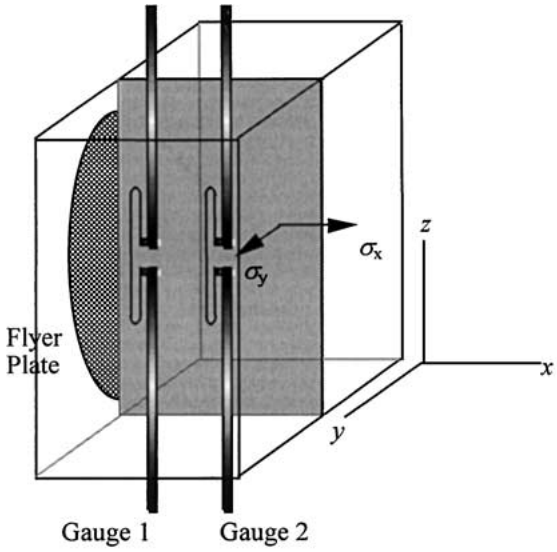

a.

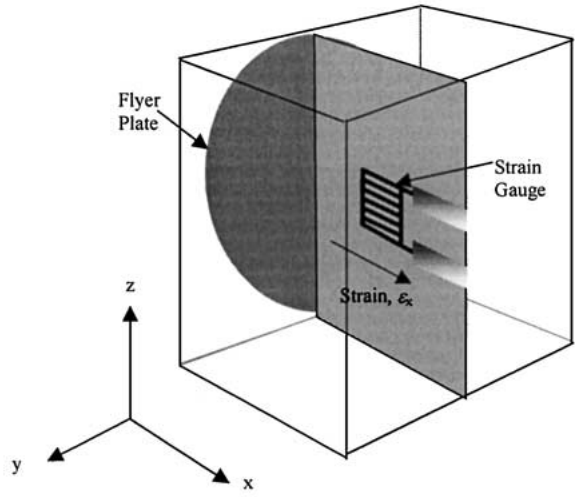

b.

Figure 1 Specimen configuration and gauge placements. (a) Lateral stress gauge, (b) Longitudinal strain gauge.

3. Materials data

The alumina used in this investigation was nominally 97.5% pure, with impurities present as grain boundary glassy phases, and a porosity of ∼3.5 volume %. The mean grain size was 4 ± 4 microns. Density (ρ_0) was 3.80 ± 0.05 g cm^{-3}, longitudinal wave speed (c_L) 10.30 ± 0.01 mm μs^{-1}, shear wave speed (c_S) 6.07 ± 0.01 mm μs^{-1} and Poisson's ratio (ν) 0.23. The HEL is 7.7 ± 0.5 GPa.

4. Results and discussion

Lateral stress histories as a function of position, at an impact stress of 9.4 GPa are presented in Fig. 2.

The temporal spacing between each gauge trace is arbitrary, and is present to aid interpretation. In the traces labeled 2 mm and 4 mm, observe that the lateral stress rises to an initial value of ∼3 GPa. After approximately 0.2 μs at 2 mm and 0.5 μs at 4 mm, the lateral stress undergoes a second increase to ∼4.5 GPa. Assuming that the longitudinal stress is constant, then from equation 3, it can be seen that this represents a delayed loss

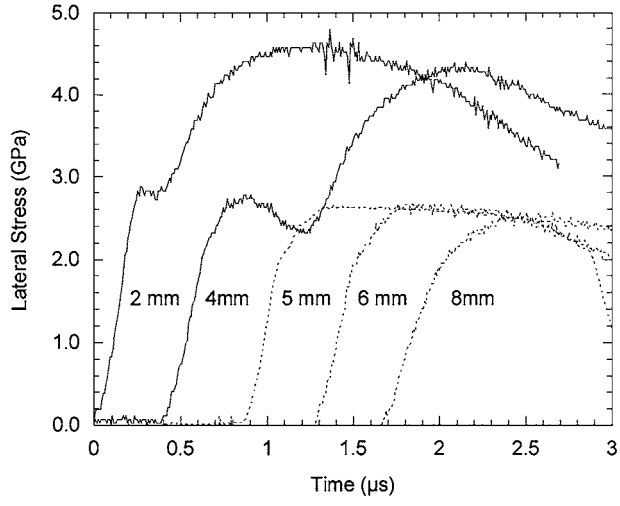

Figure 2 Lateral stress as a function of distance from the impact face. The impact stress is 9.4 GPa. Gauge positions are ±0.1 mm. Errors in measured lateral stress are ±2%. From the dimensions of the flyer plate (50 mm) and the measured wave speed ($c_L = 10.30$ mm μs^{-1}), lateral stress releases should enter the gauge location approximately 1.7 μs after the arrival of the main shock at the gauge location.

of shear strength. Such behaviour is characteristic of the failure wave phenomenon in shock loaded brittle materials. At the 4 mm position, notice that there is a dip in lateral stress before the arrival of the failure wave. Such behaviour has been observed in other shock loaded ceramics such as silicon carbide [17] and titanium diboride [19] where similar measurements have been made. The main feature of note in Fig. 2, is that the failure wave does not penetrate further than 5 mm into the target, thus indicating that the failure wave is slowing down as it moves into the target. This is in contrast to observations in silicate glasses [16], where high-speed photographic evidence shows that a constant failure wave velocity is maintained, until it is stopped by release waves from the rear of the target. Thus it would seem likely that the progress of the failure wave is impeded by something in the ceramic that is not present within glasses. The most obvious candidate would be the presence of grain boundaries. If failure within individual grains occurs down preferred orientations, then as cracks encounter differently orientated grains at grain boundaries, it is possible that some of those grains will not have orientations favorable for the transmission of fracture across those boundaries. As such behaviour is also seen in polycrystalline silicon carbide [17] and titanium diboride [19], it would seem the mostly likely cause.

In Fig. 3, we present lateral stress measurements taken 2 mm from the impact surface, at impact stresses of 6.3, 9.4 and 12.5 GPa.

Note that this figure shows that as impact stress increases, failure wave velocity also increases, as shown by the shorter time spent at the first level of lateral stress. At 12.5 GPa, lateral stress increases to a single value of ∼6.5 GPa, indicating that at this stress, failure occurs sufficiently fast that it takes place inside the shock front itself. Again this type of behaviour has been demonstrated in other materials such as a lead-filled silicate glass [31], where it was shown to occur at approximately twice the HEL, and in silicon carbide [18]. However, in the case of both the alumina studied here and the silicon carbide, the point at which failure occurs in the shock itself is significantly lower than twice the HEL.

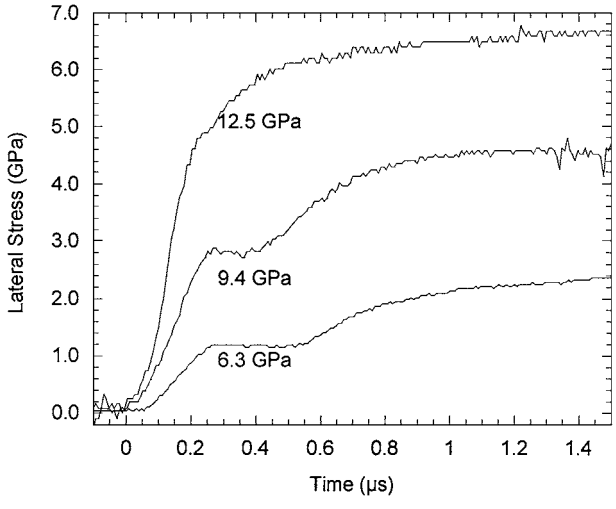

Figure 3 Lateral stress histories with increasing impact stress. Gauges are 2 mm from the impact face.

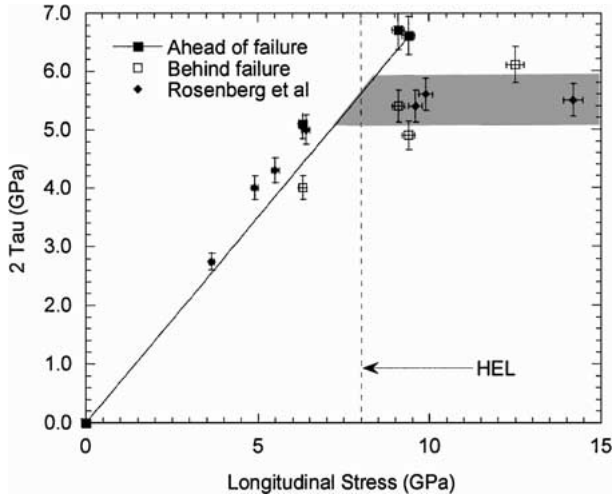

Figure 4 Shear strength as a function of impact stress. The shaded area covers the range of shear strengths measured by Munson and Lawrence [32].

In Fig. 4, we present the calculated shear strengths, both ahead of and behind the failure wave, calculated from Equation 3. In a previous paper [32], where shear strength measurements were made in a tungsten heavy alloy, we demonstrated that our results were similar to those of Zhou and Clifton [33], who measured shear strength in a similar material, using a non-invasive interformetric method. Thus we have confidence that the results in Fig. 4 represent the true mechanical response of this alumina to shock loading.

We have also included the data from Rosenberg *et al*. [34] who used the same lateral stress gauge technique in a lower purity alumina, AD 85. Observe that the degree of agreement between the two sets of data is remarkably high, given that the compositions between the two materials are quite different. Thus it would seem that the controlling factor that defines the shear strength of aluminas during one-dimensional shock loading is the alumina grains themselves, with additional factors such as additional glassy phases or porosity having a much smaller contribution. Note however that did not observe the presence of failure waves, as their gauges were mounted further back from the impact face, thus making it unlikely that the failure wave could enter the gauge location. The solid straight line is an elastic fit according to,

$$\sigma_y = \frac{\nu}{1-\nu}\sigma_x, \quad \text{and thus} \quad 2\tau = \frac{1-2\nu}{1-\nu}\sigma_x, \quad (4)$$

where ν is the Poisson's ratio. Note that the unfailed strenghts agree reasonably well with the calculated strengths according to Equation 4, even above the quoted HEL [5] of ∼7.7 GPa. This may seem surprising, but such behaviour has also been observed in silicate glasses [35]. It would seem likely that the traditional interpretation of the HEL as an elastic/plastic transition as observed in metallic materials [4] may not apply in brittle materials such as ceramics and glasses. The shaded area in Fig. 4 represents the values of shear strength

TABLE I 10 mm copper flyer plate at impact velocity *ca*. 485 m s^{-1}. Impact stress is 9.4 GPa. Lateral stresses and shear strengths as a function of distance from impact surface

Gauge Pos. mm	σ_y (ahead) GPa ±2%	σ_y (behind) GPa ±2%	2τ (ahead) GPa ±4%	2τ (ahead) GPa ±4%
2 ± 0.1	2.8	4.5	6.6	2.8
4 ± 0.1	2.7	4.3	6.7	2.7
5 ± 0.1	2.6	–	6.8	–
6 ± 0.1	2.6	–	6.8	–
8 ± 0.1	2.5	–	6.9	–

TABLE II Lateral stresses and shear strengths at 2 mm from impact

σ_x (ahead) GPa ±2%	σ_y (ahead) GPa ±2%	σ_y (behind) GPa ±2%	2τ (ahead) GPa ±4%	2τ (ahead) GPa ±4%
6.3	1.2	2.3	5.1	4
9.4	2.8	4.5	6.6	4.9
12.5	–	6.4	–	6.1

calculated by Munson and Lawrence [36], who investigated a 99.9% pure alumina. By measuring the rear surface velocity of their targets, they used a different method to obtain their results, thus,

$$\sigma_x = P + \frac{4}{3}\tau, \tag{5}$$

where P is the hydrostatic stress. However, it is clear that both our failed strengths above the HEL, and the results of Rosenberg *et al*. [34] above their quoted HEL of ∼6 GPa both agree with Munson and Lawrence [36], and again gives us confidence in our results. This result also provides further evidence that the shear strengths of aluminas are controlled by the alumina grains themselves, as we get good agreement over a wide composition range, from 85% pure to 99.9% pure. Results from the lateral stress gauge experiments are summarized in Tables I and II.

5. Conclusions

Plate impact experiments performed on a 97.5% pure alumina have shown that this material displays shock induced delayed failure—the failure wave. Results show however, that unlike silicate glasses, the failure wave velocity decreases as it moves into the target, never penetrating more than 5 mm. We believe this can be attributed to the presence of grain boundaries impeding crack growth. As impact stress increases, the failure wave velocity increases until in samples shocked to 12.5 GPa, failure occurs in the shock front itself. Measurements of the lateral stress have been used to calculate the shear strength of this material under conditions of one-dimension shock loading. Before the failure wave arrives, shear strengths agree with those calculated from knowledge of the elastic properties of this material, even when measured above the quoted HEL of ∼8 GPa. Behind the failure wave, shear strengths reach a maximum of ∼6 GPa. In all cases, our results agree with those of others, either gathered by similar gauging techniques or inferred from rear surface velocity measurements. Further, these results cover quite a wide composition range, and thus their close agreement would suggest that the shear strength of shock-loaded aluminas are mainly controlled by the strength of the alumina grains themselves.

References

1. W. H. GUST and E. B. ROYCE, *J. Appl. Phys.* **42** (1971) 276.
2. R. FENG, G. F. RAISER and Y. M. GUPTA, *J. Appl. Phys.* **83** (1998) 79.
3. D. P. DANDEKAR and P. J. GAETA, in "Shock-Wave and High-Strain-Rate Phenomena in Materials," edited by M. A. Meyers, L. E. Murr and K. P. Staudhammer (Dekker, New York, 1992) p. 1069.
4. L. DAVISON and R. A. GRAHAM, *Phys. Rep.* **55** (1979) 255.
5. N. H. MURRAY, N. K. BOURNE and Z. ROSENBERG, *J. Appl. Phys.* **84** (1998) 4866.
6. J. W. STRAEHLER, W. W. PREDEBON and B. J. PLETKA, in "High-Pressure Science and Technology – 1993," edited by S. C. Schmidt, *et al.* (AIP Press, Woodbury, NY, 1994) p. 745.
7. J. CAGNOUX and F. LONGY, in "Shock Waves in Condensed Matter 1987," edited by S. C. Schmidt and N. C. Holmes (North-Holland, New York, 1988) p. 293.
8. D. E. GRADY, *Mechanics of Materials* **29** (1998) 181.
9. D. YAZIV, Y. YESHURUN, Y. PARTOM and Z. ROSENBERG, in "Shock Waves in Condensed Matter – 1987," edited by S. C. Schmidt and N. C. Holmes (North-Holland, New York, 1988) p. 297.
10. S. V. RAZORENOV, G. I. KANEL, V. E. FORTOV and M. M. ABASEMOV, *High Press. Res.* **6** (1991) 225.
11. V. N. NIKOLAEVSKII, *Int. J. Engng. Sci.* **19** (1981) 41.
12. G. I. KANEL, S. V. RASORENOV and V. E. FORTOV, in "Shock Compression of Condensed Matter," edited by S. C. Schmidt *et al.* (Eleseiver Science Publishers BV, 1991) p. 451.
13. N. S. BRAR, Z. ROSENBERG and S. J. BLESS, *Journal de Physique IV* **Colloque C3** (1991) 639.
14. N. S. BRAR, S. J. BLESS and Z. ROSENBERG, *Appl. Phys. Letts.* **59** (1991) 3396.
15. S. J. BLESS, N. S. BRAR, G. KANEL and Z. ROSENBERG, *J. Am. Ceram. Soc.* **75** (1992) 1002.
16. N. K. BOURNE, Z. ROSENBERG and J. E. FIELD, *J. Appl. Phys.* **78** (1995) 3736.
17. N. K. BOURNE, J. C. F. MILLETT and I. PICKUP, *ibid.* **81** (1997) 6019.
18. N. BOURNE, J. MILLETT, N. MURRAY and Z. ROSENBERG, *J. Mech. Phys. Solids* **46** (1998) 1887.
19. N. K. BOURNE, G. T. GRAY III and J. C. F. MILLETT, in "Shock Compression of Condensed Matter – 1999," edited by M. D. Furnish, L. C. Chhabildas and R. S. Hixson (American Institute of Physics, Melville, NY, 2000) p. 589
20. N. K. BOURNE, Z. ROSENBERG and J. E. FIELD, *Proc. R. Soc. Lond. A* **455** (1999) 1267.
21. M. HILTL and H. NAHME, *J. Phys IV* **Colloque C3** (1997) 587.
22. Z. ROSENBERG and Y. YESHURUN, *J. Appl. Phys.* **60** (1986) 1844.
23. M. D. FURNISH and L. C. CHHABILDAS, in "Shock Compression of Condensed Mater – 1997," edited by S. C. Schmidt, D. P. Dandekar and J. W. Forbes (American Institute of Physics, Woodbury, NY, 1998) p. 501.
24. N. S. BRAR, in "Shock Compression of Condensed Matter – 1999," edited by M. D. Furnish, L. C. Chhabildas and R. S. Hixson (American Institute of Physics, Melville, NY, 2000) p. 601.
25. D. E. GRADY, in "Constitutive Laws:Theory, Experiments and Numerical Implementation," edited by A. M. Rajendran and R. C. Batra (Mauna Lani, HI, 1995) p. 35.
26. N. K. BOURNE and J. C. F. MILLETT, *J. Phys. IV* **10** (2000) 281.
27. N. K. BOURNE, Z. ROSENBERG, D. J. JOHNSON, J. E. FIELD, A. E. TIMBS and R. P. FLAXMAN, *Meas. Sci. Technol.* **6** (1995) 1462.

28. Z. ROSENBERG and Y. PARTOM, *J. Appl. Phys.* **58** (1985) 3072.
29. J. C. F. MILLETT, N. K. BOURNE and Z. ROSENBERG, *J. Phys. D. Applied Physics* **29** (1996) 2466.
30. Z. ROSENBERG, D. YAZIV and Y. PARTOM, *J. Appl. Phys.* **51** (1980) 4790.
31. N. K. BOURNE, J. C. F. MILLETT and Z. ROSENBERG, *ibid.* **80** (1996) 4328.
32. J. C. F. MILLETT, N. K. BOURNE, Z. ROSENBERG and J. E. FIELD, *ibid.* **86** (1999) 6707.
33. M. ZHOU and R. J. CLIFTON, *J. Appl. Mech.* **64** (1997) 487.
34. Z. ROSENBERG, D. YAZIV, Y. YESHURUN and S. J. BLESS, *J. Appl. Phys* **62** (1987) 1120.
35. N. K. BOURNE, J. C. F. MILLETT and J. E. FIELD, *Proc. R. Soc. Lond. A* **455** (1999) 1275.
36. D. E. MUNSON and R. J. LAWRENCE, *J. Appl. Phys.* **50** (1979) 6272.

Received 20 June 2000
and accepted 1 February 2001